Acta Cytologica

Techniques

Acta Cytologica
DOI: 10.1159/000516639

Received: December 27, 2020
Accepted: April 18, 2021
Published online: June 7, 2021

Applying Probe Electrospray Ionization Mass Spectrometry to Cytological Diagnosis: A Preliminary Study by Using Cultured Lung Cancer Cells

Yuki Morimoto[a] Takeshi Oya[b] Mayuko Ichimura-Shimizu[a] Minoru Matsumoto[b] Hirohisa Ogawa[a] Tomoko Kobayashi[a] Satoshi Sumida[a] Takumi Kakimoto[a] Michiko Yamashita[c] Chunmei Cheng[d] Koichi Tsuneyama[a, b]

[a]Department of Pathology and Laboratory Medicine, Institute of Biomedical Sciences, Tokushima University Graduate School, Tokushima, Japan; [b]Department of Molecular Medicine, Institute of Biomedical Sciences, Tokushima University Graduate School, Tokushima, Japan; [c]Department of Morphological Laboratory Science, Institute of Biomedical Sciences, Tokushima University Graduate School, Tokushima, Japan; [d]Pharmacology and Histopathology, Novo Nordisk Research Centre China, Beijing, China

Keywords
Mass spectrometry · Rapid cytological diagnosis · Probe electrospray ionization mass spectrometry · Lung cytopathology

Abstract
Objectives: Cytology and histology are 2 indispensable diagnostic tools for cancer diagnosis, which are rapidly increasing in importance with aging populations. We applied mass spectrometry (MS) as a rapid approach for swiftly acquiring nonmorphological information of interested cells. Conventional MS, which primarily rely on promoting ionization by pre-applying a matrix to cells, has the drawback of time-consuming both on data acquisition and analysis. As an emerging method, probe electrospray ionization-MS (PESI-MS) with a dedicated probe is capable to pierce sample and measure specimen in small amounts, either liquid or solid, without the requirement for sample pretreatment. Furthermore, PESI-MS is timesaving compared to the conventional MS. Herein, we investigated the capability of PESI-MS to characterize the cell types derived from the respiratory tract of human tissues. ***Study Design:*** PESI-MS analyses with DPiMS-2020 were performed on various type of cultured cells including 5 lung squamous cell carcinomas, 5 lung adenocarcinomas, 5 small-cell carcinomas, 4 malignant mesotheliomas, and 2 normal controls. ***Results:*** Several characteristic peaks were detected at around m/z 200 and 800 that were common in all samples. As expected, partial least squares-discriminant analysis of PESI-MS data distinguished the cancer cell types from normal control cells. Moreover, distinct clusters divided squamous cell carcinoma from adenocarcinoma. ***Conclusion:*** PESI-MS presented a promising potential as a novel diagnostic modality for swiftly acquiring specific cytological information.

karger@karger.com
www.karger.com/acy

Correspondence to:
Mayuko Ichimura-Shimizu, ichimura.mayuko@tokushima-u.ac.jp

Introduction

Cytology is an indispensable tool for diagnostic screening cancer and postoperative follow-up. In addition to conventional exfoliative cytology and fine-needle aspiration cytology, a new cell collection method such as endoscopic ultrasound-guided fine-needle aspiration has been developed, and its diagnostic significance is increasing. Cytology has facilitated the acquisition of cell-based morphological information by immunostaining in general. However, it is both of cost and time-consuming when multi-staining needed. To decrease cost and save time but without compromising diagnostic reliability, herein, we report a rapid mass spectrometry (MS) application to acquire additional nonmorphological diagnostic information.

MS is a highly sensitive technology that can be used for analyzing various substances. Substances are ionized using an electron beam and then could be separated based on mass differences. In clinical settings, MS has been applied to the toxicological analysis, biochemical assays, metabolites screening, and recently has been used for the rapid identification of microorganisms [1]. MS has been used to detect metabolites derived from cultured cells as well. Moreover, MS has attracted attention as a new method for biomarker identification due to its achievement in distinguishing the cell types [2–7]. Furthermore, MS application has been expanded to a comprehensive imaging analysis on tissue sections and to visualize the data 2 dimensionally for basic pathology research [8, 9]. However, certain obstacles remain unsolved in the application of MS to pathological diagnosis. A significant concern is instrument cost, which mainly prevents most hospitals from implementing MS application. Also, the optimization of pretreatment for increasing ionization efficiency and enhancement of analytical competency need to be improved.

To date, probe electrospray ionization-MS (PESI-MS) has been developed as a versatile and inexpensive technology with an exquisite probe piercing sample and at the same time spraying a voltage-based solvent to induce ionization [10]. The promising advantages of PESI-MS include the capability of measurement on a small amount of the specimen, either liquid or solid based, without the demand of sample pretreatment, and the measurement can be accomplished in a short time. Recently, PESI-MS was reported with an impressive data in which a significant difference was observed by the mass spectra of cancer tissues compared to the normal regions in a hepatocellular carcinoma model mouse [8]. In human cohorts, PESI-MS was used in the diagnosis of head and neck squamous cell carcinoma, renal cell carcinoma, breast cancer, and hepatocellular carcinoma [11–15]. Therefore, PESI-MS has been considered as a potential diagnostic application for distinguishing malignant from benign tissues. In this study, we investigated the capability of PESI-MS to characterize various types of cultured cells originally derived from human respiratory tracts.

Materials and Methods

Cultured Cell Lines

A total of 21 human cell lines were investigated: 5 of lung squamous cell carcinomas (H520, H1703, H2170, LC-A1, and H1869), 5 of lung adenocarcinomas (A549, PC9, PC14, H441, and H358), 5 of small-cell carcinomas (SBC3, SBC5, H211, H1048, and H69), and 4 of malignant mesotheliomas (Y-MESO-14, H28, H2373, and H2052). Airway epithelial cells (BEAS2B) and mesothelial cells (MeT5A) were applied as normal controls.

Cell Culture

Ten milliliter of a liquid medium containing 10% of FBS and 1% (w/v) of penicillin were added in a culture dish, and the culture medium was allowed to equilibrate in a 37°C 5% CO_2 incubator. Three types of media, BEBM (Lonza) for BEAS2B, D-MEM (Wako) were used for A549, SBC3, SBC5, and MeT5A, respectively, and RPMI1641 (Wako) was used for the rest cell lines other than the above. The medium was prepared freshly for use and cells were cultured up to 80% of confluence and then cells were treated with trypsin for collection, passage, and/or cryopreservation which was stored at −80°C.

MS Analysis

Frozen cell lines were thawed, and the supernatant was removed following centrifugation, and cells were washed in PBS 3 times. The resultant cell pellet was placed in a mass spectrometer DPiMS-2020 (Shimadzu Corporation, Kyoto, Japan) to perform PESI-MS analysis. Each sample was applied to MS 3 times (Fig. 1). The driving and analyzing condition of DPiMS-2020 were as follows: ionization position at −37 mm, ionization stop time at 200 ms, sample collection position at −46.3 mm, sample collection stop time at 50 ms, probe speed at 250 mm/s, probe acceleration at 0.63 G, DL temperature at 250°C, heat block temperature at 30°C, interface voltage at 2.45 kV (positive mode), scan speed at 5,000 u/s, scan range at m/z 10–2,000, and data collection time at 1 min (positive mode).

Data Analysis

The PESI-MS data were acquired by an elaborate software, eMSTAT Solution (Shimadzu Corp.). Multivariate analysis (partial least squares-discriminant analysis [PLS-DA]) was performed for the mass spectrum of each sample to enable two-dimensional clustering of different groups. The dataset was also processed through MetaboAnalyst 4.0, a comprehensive tool for metabolomics analysis and data interpretation (https://www.metaboanalyst.ca; RRID:SCR_015539). Mass data were uploaded as a csv file in unpaired columns and normalization was achieved by the log trans-

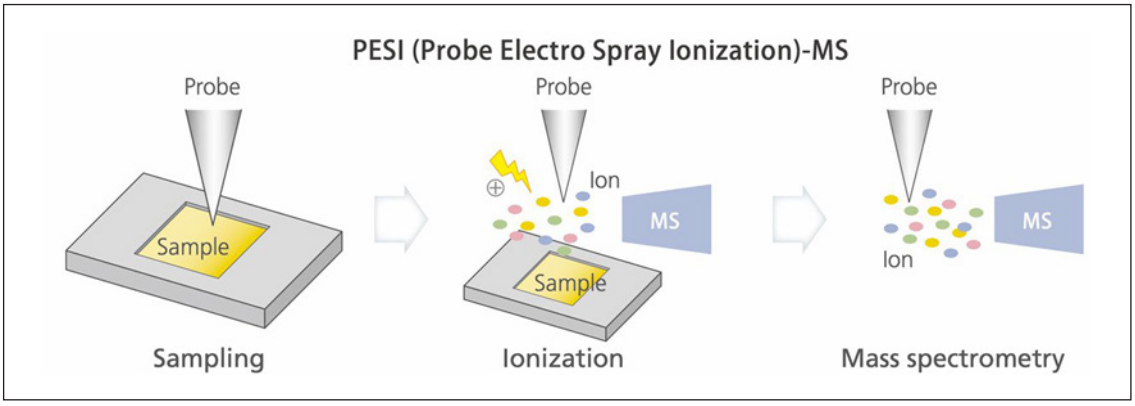

Fig. 1. Illustration of the PESI-MS mechanism and cell line analysis. PESI-MS, probe electrospray ionization mass spectrometry.

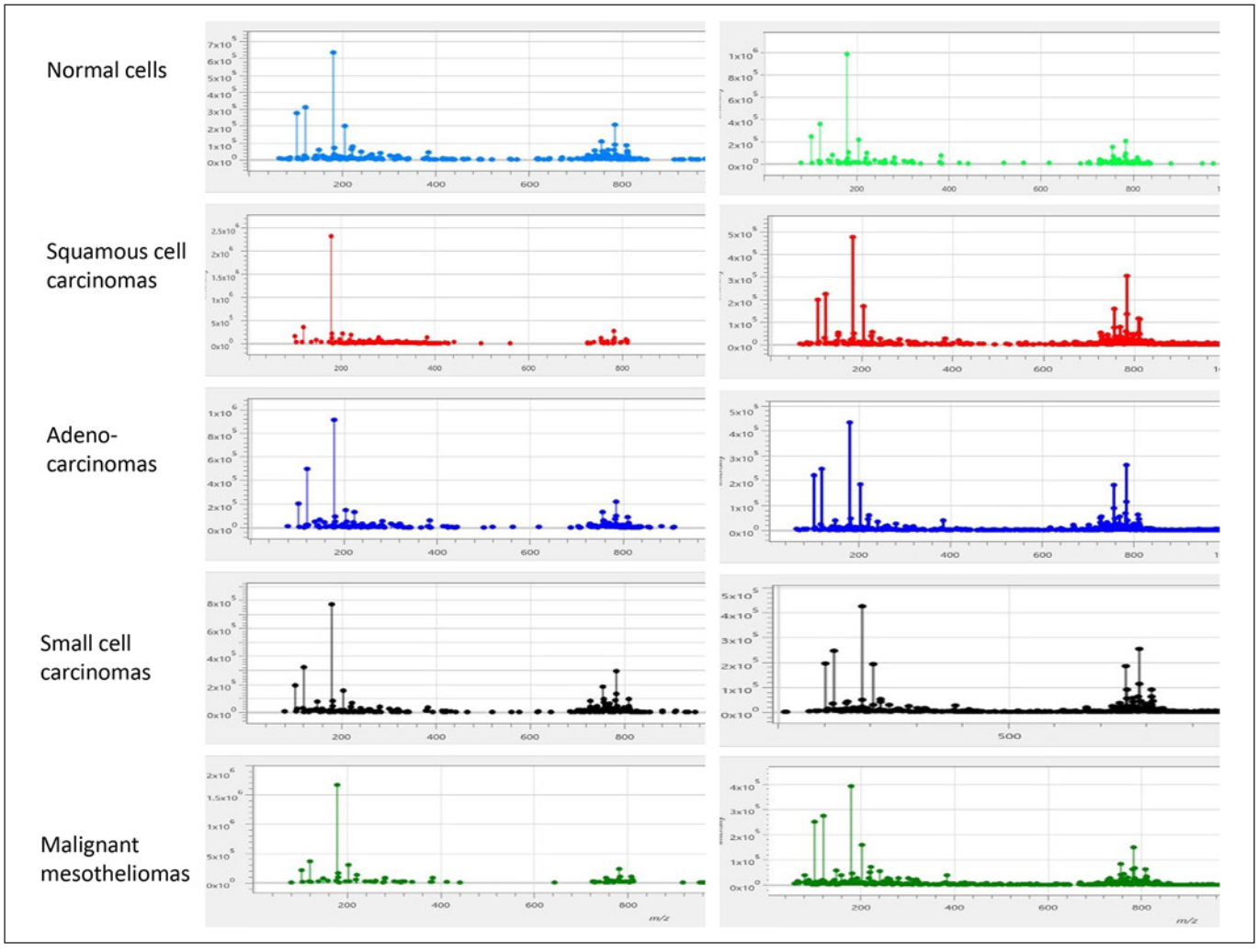

Fig. 2. Representative mass spectral patterns of each cell type. Normal cell lines, airway epithelial cell, BEAS2B and mesothelial cell, MeT5A. Lung squamous cell carcinoma cell line, H520 and H2170. Lung adenocarcinoma cell line, A549 and H441. Small-cell carcinoma cell lines, SBC3 and H1048. Malignant mesothelioma cell lines, Y-MESO-14 and H28.

Table 1. Total number of detected peaks in each sample

Origin	Cell line	Total peak	Cryopreservation period, weeks
Squamous cell carcinoma	H520	159	33
Squamous cell carcinoma	H1703	192	33
Squamous cell carcinoma	H2170	867	15
Squamous cell carcinoma	LC-A1	1,105	15
Squamous cell carcinoma	H1869	844	15
Adenocarcinoma	A549	231	35
Adenocarcinoma	PC9	246	33
Adenocarcinoma	PC14	128	33
Adenocarcinoma	H441	858	15
Adenocarcinoma	H358	897	15
Small-cell carcinoma	SBC3	326	35
Small-cell carcinoma	SBC5	346	35
Small-cell carcinoma	H211	223	33
Small-cell carcinoma	H1048	890	15
Small-cell carcinoma	H69	597	15
Malignant mesothelioma	Y-MESO-14	139	33
Malignant mesothelioma	H28	704	15
Malignant mesothelioma	H2373	770	15
Malignant mesothelioma	H2052	963	15
Benign airway epithelial cell	Met5A	167	35
Benign mesothelial cell	Beas2B	356	30

formation and auto scaling. eMSTAT conducted automatic waveform processing and missing the mass spectral value could occur when the waveform could not be detected. Setting to 1/5 of the minimum value could possibly avoid missing the mass spectral value according to the reported example of processing MetaboAnalyst [13].

Results

Each cell sample was detected by mass spectra at range of m/z 0–2,000 with DPiMS-2020. Several characteristic peaks were detected at the area around m/z 200 and 800 that were found in all samples. Representative mass spectra of normal cell lines and squamous cell carcinoma cell lines were presented in Figure 2. In this study, samples were stored at −80°C until measurement, and the cryopreservation period differed among the samples. Eleven samples (BEAS2B, MeT5A, H520, H1703, A549, PC9, PC14, SBC3, SBC5, H211, and Y-MESO-14) had a long cryopreservation period and the total number of peaks in each sample ranged from 128 to 356. In contrast, the samples with a relatively short cryopreservation duration exhibited a total number of peaks ranging from 597 to 1,105. There was a likelihood of a negative correlation between the total number of detected peaks and the cryopreservation duration (Table 1).

PLS-DA analysis was performed with the mass spectrum for each sample. The mass spectrum of each sample was displayed as a point on a graph in PLS-DA. When the distribution of plot conducted by the mass spectrum for each sample was distinct from the others, the difference among the samples was defined. In this experiment, triple mass spectra for each sample were plotted concurrently. The identification of malignant cells was determined by the distinct plots' distribution from that of normal cells (Fig. 3). The mass spectrum of BEAS2B, a normal airway epithelial cell line, was plotted at the top of the graph, and the mass spectrum of cancer cells, groups of squamous cell carcinoma, adenocarcinoma, and small-cell carcinoma was plotted at the bottom of the chart (Fig. 3a–c). A similar tendency was confirmed on MeT5A, which was a normal mesothelial cell line. MeT5A was distinguished from each type of cancers, including malignant mesothelioma, although several plots of malignant cells were difficult to cut off from normal cells (Fig. 3d–g).

The data were then analyzed by contrasting each tissue type to verify among the distinguished tissue types (Fig. 4). We then compared the metabolites (m/z) between those of squamous cell carcinoma and adenocarcinoma. Among the differently expressed metabolites identified by PESI-MS, only the top 25 metabolites were se-

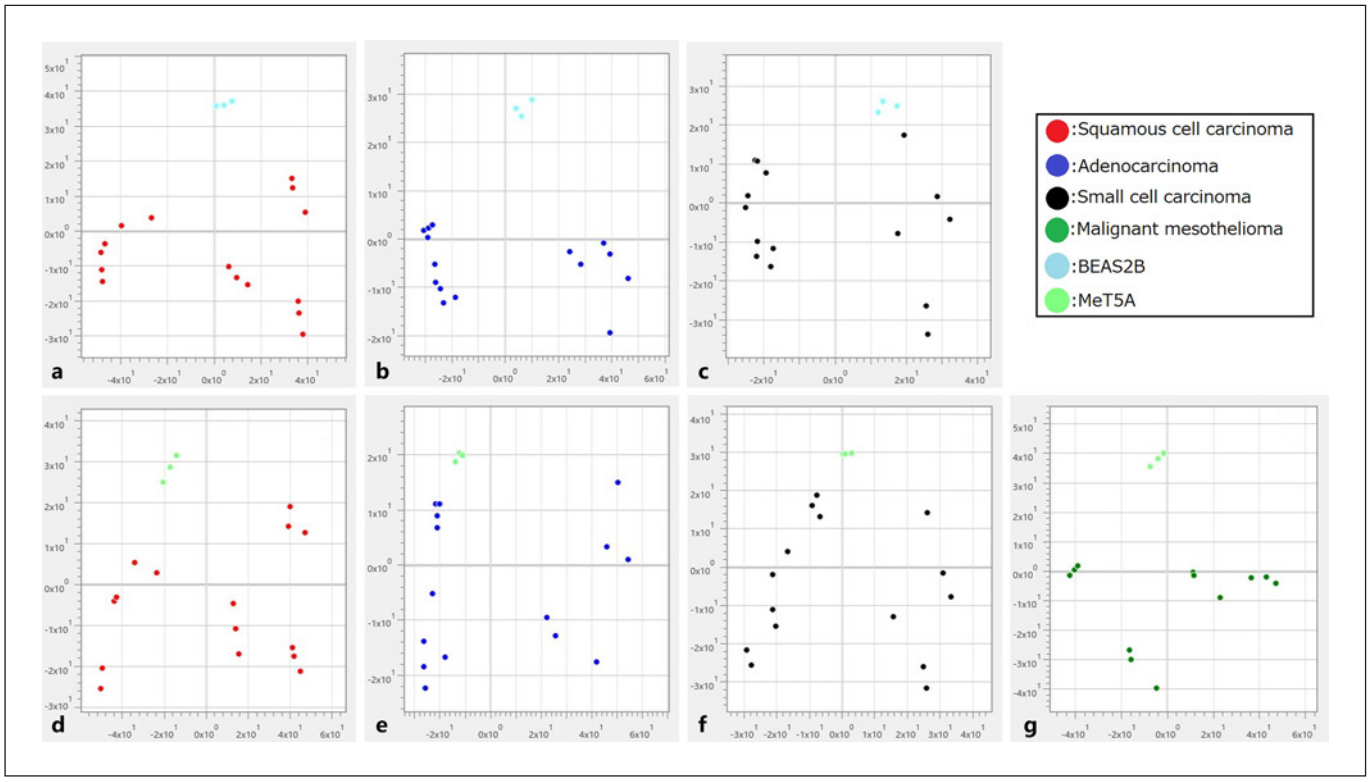

Fig. 3. Differences in mass spectra of normal and cancer cells by PLS-DA analysis. **a** Airway epithelial cell versus squamous cell carcinoma. **b** Airway epithelial cell versus adenocarcinoma. **c** Airway epithelial cell versus small-cell carcinoma. **d** Mesothelial cell versus squamous cell carcinoma. **e** Mesothelial cell versus adenocarcinoma. **f** Mesothelial cell versus small-cell carcinoma. **g** Mesothelial cell versus malignant mesothelioma. PLS-DA, partial least squares-discriminant analysis.

lected and constructed into a heat map (Fig. 5). The heat map exhibited the distinctive patterns of metabolites between squamous cell carcinoma and adenocarcinoma. The volcano plots highlighted metabolites with a raw p value <0.05 ($p < 0.05$) and fold change of threshold greater than 2 in adenocarcinoma/squamous cell carcinoma ratio (Fig. 6a). Those of top 26 to 50 metabolites highlighted by the volcano plots distinguishing each cell type but with a low p value, as candidates were listed in Table 2. For example, selected boxplot of metabolites, m/z 1,569.28 is a candidate for distinguishing squamous cell carcinoma from adenocarcinoma (Fig. 6b).

Discussion

Pathologic diagnosis is primarily based on the morphology of cells and tissues. Cytopathology is an alternative approach to evaluate the tissue origin from exfoliated cells based on the cell-specific morphology. However, the bias and variation of morphological analysis amongst cytopathologists have brought up the subjective argument. Therefore, a double-check system by multiple cytopathologists was recommended in clinical settings. While that significantly reduced subjective bias, cytopathologists have been bearing the redundant workload for it. Recently, the application of using artificial intelligence for auxiliary morphological diagnosis has progressed [16], however, this approach is still morphology dependent. A morphology-independent technology for assessing tissues and cells is yeaned to develop for complementary to current diagnostic approach. MS is a technology to enable the identification of substances contained in tissues and cells. Due to emerging technology innovations, MS has been widely applied in the medical field. Besides the particular benefits of MS, both sample pretreatment for ionizing targets and data analysis are time-consuming. Moreover, the expensive cost of detection devices hinders the application of MS in pathological and cytological diagnosis. In this study, we investigated the applicability of

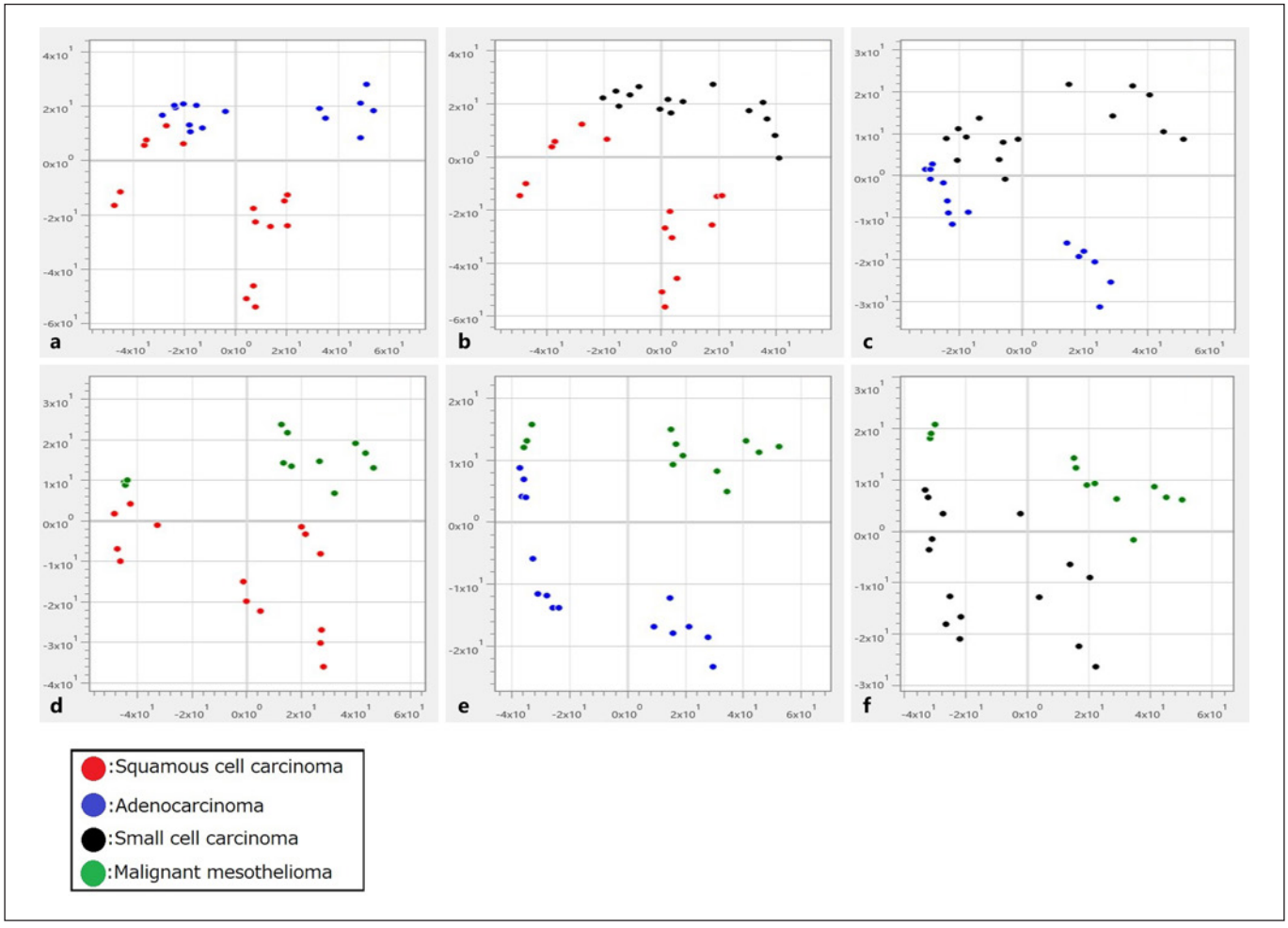

Fig. 4. Differences in mass spectra of various tissue types by PLS-DA analysis. **a** Squamous cell carcinoma versus adenocarcinoma. **b** Squamous cell carcinoma versus small-cell carcinoma. **c** Adenocarcinoma versus small-cell carcinoma. **d** Squamous cell carcinoma versus malignancy mesothelioma. **e** Adenocarcinoma versus malignant mesothelioma. **f** Small-cell carcinoma versus malignant mesothelioma. PLS-DA, partial least squares-discriminant analysis.

a rapid mass spectrometer (PESI-MS) in cytological diagnosis. In operation, PESI-MS is a relatively easier and faster than conventional MS. In addition, the detection device of PESI-MS is cheaper than those of conventional MS, making it well suited in clinical settings. Because of different ionization methods, detectable substances with conventional MS may not be able to detect by PESI-MS, therefore, it is pivotal to validate the reliability of data generated by PESI-MS. We investigated the feasibility and reliability of PESI-MS in cytology application by analyzing various cultured cell lines originally derived from the human respiratory system. As expected, distinctive mass spectra of various cultured cell lines were swiftly detected by PESI-MS. Particularly, PESI-MS could distinguish the benign cells from malignant ones, as well as distinguish different histological types. Notably, some specific peaks such as m/z 1,569.28 were able to discriminate the squamous cell carcinoma from the adenocarcinoma. In the positive mode, the masses of sodium, potassium, and hydrogen ions were added, and in the negative mode, they were omitted. The actual candidate substance was expected to have a value smaller than m/z 1,569.28. However, the identified peak (m/z 1,569.28) was not registered in the human metabolome database even several species of major ion adduct were taken into consideration. Nevertheless, the strategy directed here showed the possibility of the identification of novel biomarkers.

This indicated that coupling MS data to morphological analyses enables the improvement of the quality and capacity of pathological diagnosis. Furthermore, intracel-

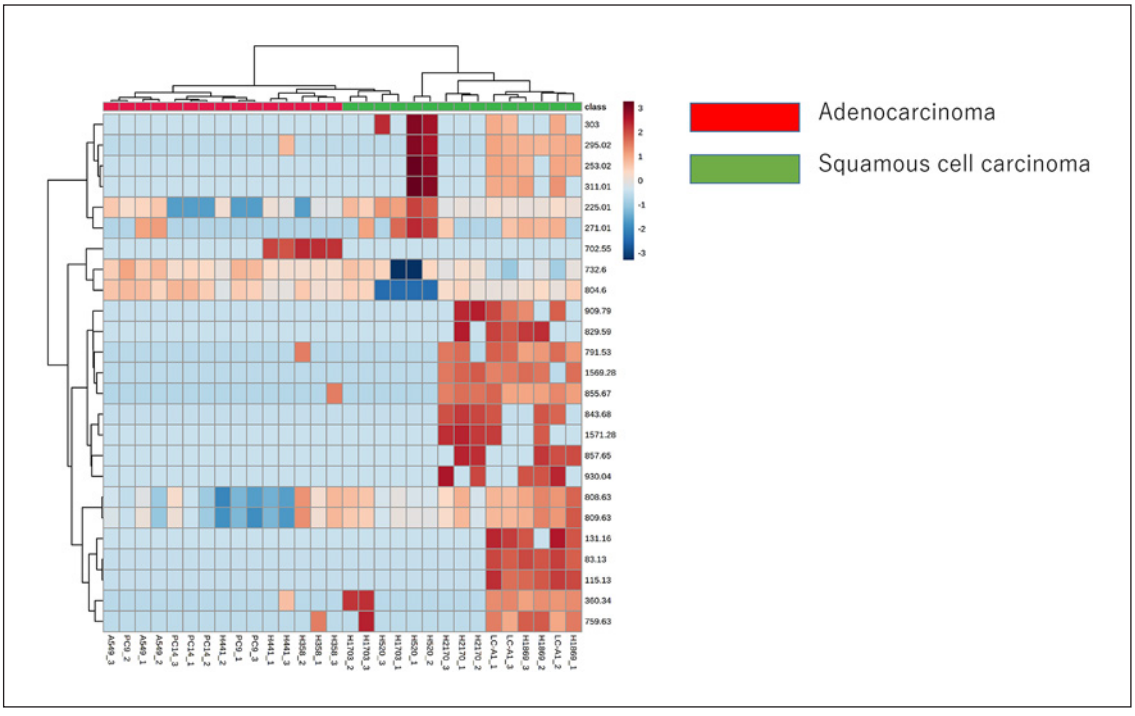

Fig. 5. Heatmap of identified metabolites (m/z) showing the 25 differentially expressed metabolites between squamous cell carcinoma and adenocarcinoma with the smallest *t* test *p* values. Euclidean distance metric and Ward's clustering method was used for the hierarchical clustering of samples.

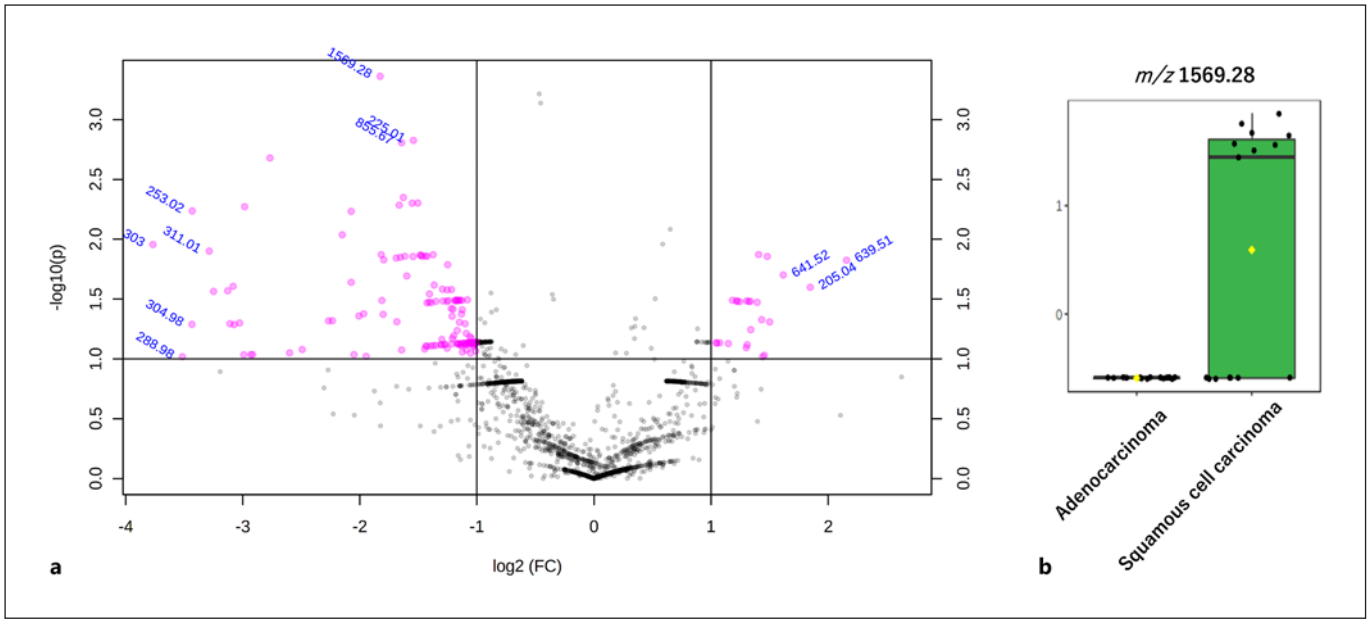

Fig. 6. a The volcano plots highlight metabolites with raw *p* values <0.05 and fold change threshold >2 in adenocarcinoma/squamous cell carcinoma ratio. The volcano plots highlight candidate metabolites distinguishing each cell type. For example, selected boxplot of metabolites, m/z 1,569.28 is a candidate to differentiate squamous cell carcinoma from adenocarcinoma (**b**).

Table 2. Top 50 features identified by fold change analysis

	Peaks, m/z	FC	$\log_2$ (FC)	Raw *p* value	$-\log_{10}$ (*p* value)
1	1,569.28	0.28192	−1.8266	0.000435	3.3615
2	225.01	0.34331	−1.5424	0.001493	2.8261
3	855.67	0.32011	−1.6433	0.00156	2.8068
4	360.34	0.14684	−2.7677	0.002093	2.6793
5	791.53	0.32344	−1.6284	0.004478	2.3489
6	83.13	0.35225	−1.5053	0.004977	2.303
7	843.68	0.34081	−1.553	0.004994	2.3015
8	115.13	0.31555	−1.6641	0.005184	2.2853
9	295.02	0.12642	−2.9838	0.005344	2.2721
10	253.02	0.092669	−3.4318	0.005798	2.2368
11	909.79	0.23756	−2.0736	0.005844	2.2333
12	271.01	0.22531	−2.15	0.009182	2.0371
13	303	0.073433	−3.7674	0.011068	1.9559
14	311.01	0.10248	−3.2866	0.012556	1.9011
15	702.55	2.6493	1.4056	0.013427	1.872
16	759.63	0.28382	−1.817	0.013451	1.8712
17	857.65	0.38585	−1.3739	0.013477	1.8704
18	1,571.28	0.35743	−1.4843	0.013553	1.868
19	829.59	0.35918	−1.4772	0.013609	1.8662
20	131.16	0.36848	−1.4404	0.013815	1.8597
21	930.04	0.3725	−1.4247	0.013864	1.8581
22	839.65	0.32631	−1.6157	0.013876	1.8577
23	454.7	0.36107	−1.4696	0.013893	1.8572
24	1,155.73	2.7884	1.4794	0.013916	1.8565
25	892.66	0.34254	−1.5456	0.013953	1.8553
26	949.6	0.31769	−1.6543	0.014164	1.8488
27	835.58	0.30999	−1.6897	0.014352	1.8431
28	1,040.37	0.288	−1.7959	0.014846	1.8284
29	639.51	4.4581	2.1564	0.01498	1.8245
30	860.6	0.42051	−1.2498	0.016331	1.787
31	641.52	3.0661	1.6164	0.019887	1.7014
32	1,570.2	0.33015	−1.5988	0.020262	1.6933
33	251.01	0.2375	−2.074	0.022922	1.6398
34	167.08	0.38809	−1.3656	0.024135	1.6174
35	325.04	0.11808	−3.0822	0.024744	1.6065
36	205.04	3.5969	1.8468	0.025227	1.5981
37	458.82	0.40753	−1.295	0.026176	1.5821
38	302.18	0.43014	−1.2171	0.026337	1.5794
39	149.05	0.41924	−1.2541	0.026516	1.5765
40	229.01	0.11435	−3.1285	0.026973	1.5691
41	265.04	0.10515	−3.2494	0.027297	1.5639
42	69.27	0.37744	−1.4057	0.028664	1.5427
43	751.51	0.47261	−1.0813	0.032067	1.4939
44	426.74	0.4392	−1.187	0.032298	1.4908
45	153.03	0.444	−1.1714	0.032304	1.4907
46	576.57	0.45289	−1.1428	0.032375	1.4898
47	634.59	0.44329	−1.1737	0.032389	1.4896
48	678.49	2.2683	1.1816	0.032396	1.4895
49	1,535.18	0.44754	−1.1599	0.032423	1.4891
50	189.03	0.45781	−1.1272	0.032439	1.4889

lular metabolites such as lipids and amino acids, which are generally unable to be identified by conventional pathological techniques, could be detected by PESI-MS. This may lead to the discovery of novel diagnostic markers based on the unique patterns of mass spectra of tissue types. Further back-to-back studies such as MS/MS analysis are necessary to identify the substances detected by PESI-MS herein. Currently, by combining with other methods we are identifying the candidate substances which could define the characteristics of cells.

On the other hand, certain issues remained in PESI-MS application to cytology assessments, such as the status of sample storage before measurement. In this study, the samples were stored frozen before measurement and then were performed the analyses in one session as required. Considered various sample storage duration, the likelihood of a negative correlation between the sample storage duration and the number of detected peaks was implied. The possible reason for small number of detected peaks in samples with a long cryopreservation period was speculated that the cells were disrupted during cryopreservation and resulted in intracellular substances leaking out of the cell and being washed away by PBS. Therefore, it is recommended to apply MS on clinical samples immediately after collection. Liquid-based cytology, which is currently widespread in use on the sample with long period of storage at room temperature, is expected to apply for PESI-MS analysis.

Another challenge for PESI-MS application in cytology is to detect small numbers of atypical cells in the specimen containing a large number of normal cells. Most specimens submitted for cytological diagnosis in clinical practice contained a large number of normal cells such as red blood cells, white blood cells, and normal epithelial cells, but a small number of atypical cells. In this kind of scenario, the signals from abnormal cells might be buried in the signals from normal cells, especially in the specimens with high viscosity such as cervical smear or sputum. Also, noncellular components such as mucus raising the concern that peaks from noncellular components may obscure the cellular peaks. In fact, there are reports that the number of tumor cells in the sample affects the mass spectrum [17]. Therefore, to obtain the distinct peaks derived from atypical cells by PESI-MS for cytological diagnosis requires a pretreatment to remove normal cells and noncell components as much as possible before measurement.

PESI-MS has been effectively applied in rapid on-site evaluation (ROSE) of cytological samples for cytological diagnosis [18]. Since most specimens for ROSE were collected from tumor regions, the proportion of tumor cells in the sample was generally high. The greater proportion of tumor cells in a specimen, the easier it is to detect distinct mass spectra from tumor cells compared to that from normal cells. PESI-MS application to ROSE for cytological diagnosis provided a practical solution to enhance the tumor specificity. The conventional histological evaluation requires 5 steps to reach the achievement, namely: (1) specimen collection, (2) smearing, (3) fixation, (4) staining, and (5) microscopic examination. In comparison, PESI-MS only requires 2 steps: (1) collection and (2) measurement. Moreover, the measurement of PESI-MS is more efficient on difficult-to-distinguish cells in a specimen. It has been reported that mass spectra could be detected at a single-cell level from microdissected samples using a refined ionization technology with PESI-MS [19]. PESI-MS with this developed technology enables collecting individual cells and cell clumps but only detecting mass spectra of target cells.

Deep learning belongs to machine learning technology and allows analyzing the entire mass spectrum data rather than assessing individual substances. Deep learning has been widely utilized for analyzing massive information of mass spectrum data. By accumulating mass spectrum data linked to clinical and pathomorphological information, it has the potential to classify samples according to disease features and their unique mass spectrum [20]. Furthermore, the development of PESI-MS probes could lead to a revolution of novel medical device that can be attached to endoscope or other diagnostic equipment to ensure more accurately reaching tissues or cells in the body. Rapid MS in the future could be applied simultaneously with tissue sampling, and MS information could be collected along with morphological evaluation during diagnosis.

Taken together, this study represented here a pioneering perspicacity with a great potential for applying rapid MS by PESI-MS toward pathological and cytological diagnosis. Further investigation will be taken by applying PESI-MS on the specimens preserved for liquid-based cytology in clinical practice to further prove the concept.

Acknowledgements

We would like to express our gratitude to Prof. Yasuhiko Nishioka and Dr. Hirokazu Ogino in the department of respiratory medicine and rheumatology, graduate school of biomedical sciences, Tokushima university for the donation of culture cells, and Dr. Hidekazu Saiki of Shimadzu Corporation who led the PESI-MS operation.

Statement of Ethics

In this study, we used culture cells of human origin that are commercially available and did not use samples newly collected from patients. No genetic manipulation was performed. No animal experiments have been conducted.

Conflict of Interest Statement

The authors have no conflicts of interest to declare.

Funding Sources

This work was supported by JSPS KAKENHI Grant-in-Aid for Scientific Research (A) number 17H00881 and (C) number 18K07069.

Author Contributions

Yuki Morimoto designed and executed experiments. Mayuko Ichimura-Shimizu supervised entire experiments including statistics. Takeshi Oya, Minoru Matsumoto, Hirohisa Ogawa, Tomoko Kobayashi, Satoshi Sumida, Takumi Kakimoto, and Michiko Yamashita participated in data analyses and contributed the specialty of expertise, respectively. Chunmei Cheng contributed to the perspective in developing a novel modality in cytodiagnosis and edition of the manuscript. Koichi Tsuneyama provided research funds, supervised the entire research, and conducted the manuscript.

References

1 Bizzini A, Durussel C, Bille J, Greub G, Prod'hom G. Performance of matrix-assisted laser desorption ionization-time of flight mass spectrometry for identification of bacterial strains routinely isolated in a clinical microbiology laboratory. J Clin Microbiol. 2010 May;48(5):1549–54.
2 Jia Z, Zhang H, Ong CN, Patra A, Lu Y, Lim CT, et al. Detection of lung cancer: concomitant volatile organic compounds and metabolomic profiling of six cancer cell lines of different histological origins. ACS Omega. 2018 May 31;3(5):5131–40.
3 Huang H, Tong TT, Yau L-F, Chen C-Y, Mi J-N, Wang JR, et al. LC-MS based sphingolipidomic study on A549 human lung adenocarcinoma cell line and its taxol-resistant strain. BMC Cancer. 2018;18:799.
4 Alazzo A, Al-Natour MA, Spriggs K, Stolnik S, Ghaemmaghami A, Kim DH, et al. Investigating the intracellular effects of hyperbranched polycation-DNA complexes on lung cancer cells using LC-MS-based metabolite profiling. Mol Omics. 2019 Feb 11;15(1):77–87.
5 Lim SL, Jia Z, Lu Y, Zhang H, Ng CT, Bay BH, et al. Metabolic signatures of four major histological types of lung cancer cells. Metabolomics. 2018 Aug 31;14(9):118.
6 Li W, Zhang W, Deng W, Zhong Y, Zhang Y, Peng Z, et al. Quantitative proteomic analysis of mitochondrial proteins differentially expressed between small cell lung cancer cells and normal human bronchial epithelial cells. Thorac Cancer. 2018 Nov;9(11):1366–75.
7 Sappington D, Helms S, Siegel E, Penney RB, Jeffus S, Bartter T, et al. Diagnosis of lung tumor types based on metabolomic profiles in lymph node aspirates. Cancer Treat Res Commun. 2018;14:1–6.
8 Kriegsmann K, Longuespée R, Hundemer M, Zgorzelski C, Casadonte R, Schwamborn K, et al. Combined immunohistochemistry after mass spectrometry imaging for superior spatial information. Proteomics Clin Appl. 2019 Jan;13(1):e1800035.
9 Berghmans E, Van Raemdonck G, Schildermans K, Willems H, Boonen K, Maes E, et al. MALDI mass spectrometry imaging linked with top-down proteomics as a tool to study the non-small-cell lung cancer tumor microenvironment. Methods Protoc. 2019 May 28;2(2):44.
10 Yoshimura K, Chen LC, Yu Z, Hiraoka K, Takeda S. Real-time analysis of living animals by electrospray ionization mass spectrometry. Anal Biochem. 2011 Oct 15;417(2):195–201.
11 Yoshimura K, Mandal MK, Hara M, Fujii H, Chen LC, Tanabe K, et al. Real-time diagnosis of chemically induced hepatocellular carcinoma using a novel mass spectrometry-based technique. Anal Biochem. 2013 Oct 1;441(1):32–7.
12 Yoshimura K, Chen LC, Mandal MK, Nakazawa T, Yu Z, Uchiyama T, et al. Analysis of renal cell carcinoma as a first step for developing mass spectrometry-based diagnostics. J Am Soc Mass Spectrom. 2012 Oct;23(10):1741–9.
13 Ashizawa K, Yoshimura K, Johno H, Inoue T, Katoh R, Funayama S, et al. Construction of mass spectra database and diagnosis algorithm for head and neck squamous cell carcinoma. Oral Oncol. 2017 Dec;75:111–9.
14 Iwano T, Yoshimura K, Inoue S, Odate T, Ogata K, Funatsu S, et al. Breast cancer diagnosis based on lipid profiling by probe electrospray ionization mass spectrometry. Br J Surg. 2020 May;107(6):632–5.
15 Giordano S, Takeda S, Donadon M, Saiki H, Brunelli L, Pastorelli R, et al. Rapid automated diagnosis of primary hepatic tumour by mass spectrometry and artificial intelligence. Liver Int. 2020 Dec;40(12):3117–24.
16 Coudray N, Ocampo PS, Sakellaropoulos T, Narula N, Snuderl M, Fenyö D, et al. Classification and mutation prediction from non-small cell lung cancer histopathology images using deep learning. Nat Med. 2018 Oct;24(10):1559–67.
17 Sakamoto K, Fujita Y, Chikamatsu K, Tanaka S, Takeda S, Masuyama K, et al. Ambient mass spectrometry-based detection system for tumor cells in human blood. Transl Cancer Res. 2018;7(3):758–64.
18 Baram D, Garcia RB, Richman PS. Impact of rapid on-site cytologic evaluation during transbronchial needle aspiration. Chest. 2005 Aug;128(2):869–75.
19 Chen F, Lin L, Zhang J, He Z, Uchiyama K, Lin JM. Single-cell analysis using drop-on-demand inkjet printing and probe electrospray ionization mass spectrometry. Anal Chem. 2016 Apr 19;88(8):4354–60.
20 Behrmann J, Etmann C, Boskamp T, Casadonte R, Kriegsmann J, Maaß P. Deep learning for tumor classification in imaging mass spectrometry. Bioinformatics. 2018 Apr 1;34(7):1215–23.